A prokaryotic viral sequence is expressed and conserved in mammalian brain

Yang-Hui Yeh[a], Vignesh Gunasekharan[a], and Laura Manuelidis[a,1]

[a]Section of Neuropathology, Yale University Medical School, New Haven, CT 06510

Edited by Günter Blobel, HHMI at the Rockefeller University, New York, NY, and approved May 25, 2017 (received for review April 12, 2017)

A natural and permanent transfer of prokaryotic viral sequences to mammals has not been reported by others. Circular "SPHINX" DNAs <5 kb were previously isolated from nuclease-protected cytoplasmic particles in rodent neuronal cell lines and brain. Two of these DNAs were sequenced after Φ29 polymerase amplification, and they revealed significant but imperfect homology to segments of commensal *Acinetobacter* phage viruses. These findings were surprising because the brain is isolated from environmental microorganisms. The 1.76-kb DNA sequence (SPHINX 1.8), with an iteron before its ORF, was evaluated here for its expression in neural cells and brain. A rabbit affinity purified antibody generated against a peptide without homology to mammalian sequences labeled a nonglycosylated ∼41-kDa protein (spx1) on Western blots, and the signal was efficiently blocked by the competing peptide. Spx1 was resistant to limited proteinase K digestion, but was unrelated to the expression of host prion protein or its pathologic amyloid form. Remarkably, spx1 concentrated in selected brain synapses, such as those on anterior motor horn neurons that integrate many complex neural inputs. SPHINX 1.8 appears to be involved in tissue-specific differentiation, including essential functions that preserve its propagation during mammalian evolution, possibly via maternal inheritance. The data here indicate that mammals can share and exchange a larger world of prokaryotic viruses than previously envisioned.

circular viral DNA | maternal inheritance | microbiome | synaptic boutons | evolution

The transfer of highly conserved nucleic acid sequences between elementary life-forms and mammalian species has only begun to be explored at the molecular level. The first examples of permanently incorporated lower life-forms in mammals are mitochondria. These complex organelles reside in the cytoplasm and are maternally inherited. Mitochondria derive from engulfed prokaryotes (1), an endosymbiotic concept subsequently solidified by sequencing homologies (2). Mitochondria contain a protected circular DNA genome of 16 kb, the only known cytoplasmic endosymbiont inherited through generations. They provide essential cellular functions such as the production of energy via ATP, and they perform in concert with, and are codependent on, nuclear genomic transcripts. Although some prokaryotes and many viruses can penetrate and be maintained within the cytoplasm of mammalian cells and tissues for a lifetime, they are not normally transmitted from the oocyte or sperm to their progeny. The majority are infectious pathogens, although some can be maintained in a latent or hidden state without inducing obvious disease. Examples include quiescent tubercle bacilli arrested in lymphatic macrophages, DNA viruses such as the Epstein-Barr and papova viruses, and RNA myxo-paramyxoviruses. In humans, both the JC papova viral DNA and measles viral structures have been detected incidentally in normal brain (3, 4). Nevertheless, the rare transfer of these infectious agents to germline cells, especially with progressive dissemination to normal offspring, stands in sharp contrast to the conserved cytoplasmic perpetuation of mitochondrial DNA. Indeed, the intergenerational transmission of other environmental DNAs or RNAs by maternal cytoplasmic inheritance has not been reported in mammals. The data here demonstrate that a commensal circular cytoplasmic DNA is propagated and expressed in various mammalian cells, including neurons and pancreatic insulin-secreting cells. This implicates archaic symbiotic functions.

Even in the nucleus, where episomal DNA viruses replicate and can reside for years, integration into nuclear DNA in the germline is rare. RNA retroviruses that integrate their cDNA via reverse transcriptase are the major exception. Numerous copies of long interspersed repeat elements (known as LINES) were initially isolated from human and mouse nuclear DNA, shown to be homologous with each other, and organized together in megabase Giemsa-band domains on chromosome arms (5–7). Their long ORFs suggested transcriptional and functional potentials that became clear only with the subsequent sequencing of contemporary epidemic retroviral isolates. Although the function of LINES remains incomplete, truncated to full-length transcripts are highly expressed in mammalian brain. Such elements, including lower copy human endogenous retroviruses, once established in the genome, can reintegrate into nuclear DNA and spread with increasing representation to define and organize large cohesive tissue-specific and other selected gene families (8–10). On an evolutionary scale, some xenotropic retroviruses may be selected because they are not pathogenic for their host, but can kill closely related competitive species in their local environment (8). The incorporation of retroviruses in *Drosophila* and plants (11) further emphasizes ancient molecular exchanges with environmental viruses. The recent demonstration that the ubiquitous human herpesvirus 6 can integrate into germline chromosomal telomeres in ∼1% of children also reveals ongoing nascent viral transfers, with reactivation and transmission to others via transfusion and transplantation (12, 13).

We proposed that commensal and/or environmental viruses might initiate or be involved in late-onset neurodegenerative diseases (14). Data in transmissible encephalopathies (TSEs),

Significance

Circular SPHINX DNAs with significant homology to segments of *Acinetobacter* phage viruses were previously isolated from cytoplasmic particles in mammalian cells and brain. *Acinetobacter* are widespread opportunistic pathogens, and permanent transfer of prokaryotic viruses to mammals has not been reported. To find whether 324-aa ORF of SPHINX is translated into its cognate protein (spx1), an antibody was raised against an internal peptide with no homology to any known mammalian cellular or viral sequences. Western blots of cells and brains (rodent and human) displayed antigen-specific spx1 protein in cultured cells where spx1 was perinuclear. In brain, the protein concentrated in terminal synaptic boutons. Because brain is environmentally isolated, this SPHINX element is an antediluvian symbiont probably involved in sophisticated neural functions.

Author contributions: Y.-H.Y., V.G., and L.M. designed research; Y.-H.Y., V.G., and L.M. performed research; Y.-H.Y., V.G., and L.M. analyzed data; and L.M. wrote the paper.

The authors declare no conflict of interest.

This article is a PNAS Direct Submission.

[1]To whom correspondence should be addressed. Email: laura.manuelidis@yale.edu.

This article contains supporting information online at www.pnas.org/lookup/suppl/doi:10.1073/pnas.1706110114/-/DCSupplemental.

such as human Creutzfeldt-Jakob disease (CJD) and sheep scrapie, strongly suggest that they are caused by an infectious agent that induces neurodegeneration and host prion protein (PrP) amyloid after a prolonged infectious, but clinically silent period (14). A subset of amyloid and other protein misfolding diseases, such as postencephalitic Parkinson's disease, have a viral history, and measles infections can also induce neurofibrillary tangles that are indistinguishable from those seen in Alzheimer's disease brain (e.g., ref. 15). The eradication of human kuru and the dramatic reduction of epidemic U.K. cow TSE were achieved by removing infectious material. In addition, substantial agent strain, PrP recombinant, and recent nucleic acid data (14, 16, 17) together indicate a still-unresolved causal protected environmental virus. The cytoplasm of CJD- and scrapie-infected cells, but not control cells, also contains virus-like particle arrays (18), and because we were able to isolate these nuclease-protected particles with quantitative recovery of infectivity, but with little or no detectable PrP (17, 19), we began to analyze protected nucleic acids. Using Φ29 rolling circle amplification, several circular DNA sequences of <5 kb with ORFs were thereby discovered in brain and cultured neuronal cell lines. These circular DNA sequences were named SPHINX elements for their initial association with slow progressive hidden infections of X origin (20). They had no homology to mammalian nuclear or mitochondrial DNA, but had significant nucleotide homology ($<10^{-105}$, 70%) to replication initiation viral regions of *Acinetobacter*, a wound pathogen that is common in soil and water (20). The bacterial virus is typically ∼12 kb, and bacterial DNA was not detectable, nor were SPHINX DNAs found in any reagents used. Subsequently, the SPHINX DNAs were independently isolated in Europe from human multiple sclerosis brains, cow milk, and serum (21, 22), and additional PCR studies here revealed SPHINX DNAs were present in uninfected samples, and thus may not be the sole causal TSE agent (17). Their unique cytoplasmic residence, strong bacteriophage homology, and potential mammalian functions, especially in brain, impelled further study.

We here focus on the SPHINX 1.8 DNA translation into protein and its representation in cultured neuronal GT1 cells, and in control versus TSE brain samples with severe end-stage neurodegeneration (e.g., refs. 14 and 23). To find whether the SPHINX 1.8 DNA was processed into its 324-aa cognate protein (spx1), rabbit antibodies were raised against selected ORF peptides that had no homology with any mouse, human, or other known mammalian nuclear or cytoplasmic sequence in the database. Two rabbit antisera, as well as an affinity-purified antibody, cleanly bound a blotted 41-kDa protein band close to its predicted 37.3-kDa mass; antibody binding was completely blocked by its immunogenic peptide. This 41-kDa spx1 band is expressed not only in cultured cells exposed to bovine serum, but also is obvious in environmentally isolated brain samples removed sterilely from different mammalian species that included wild-type (wt) and transgenic mice, Syrian hamsters, and human brain-glioblastoma samples. Most remarkably, in situ studies revealed a very high signal intensity of spx1 in synaptic boutons innervating anterior motor horn neurons, as well as in pancreatic islet, but not exocrine, cells. Together, the results here indicate spx1 can have a fundamental role in cellular differentiation, neoplasia, and synaptic neural function. Protected cytoplasmic SPHINX DNA particles are probably the tip of the iceberg of DNAs originating from symbiotic prokaryotic viral sequences in the environment that are conserved in mammalian evolution.

Results

Cytoplasmic SPHINX DNAs were originally detected only after removing >99.5% of nuclear DNA followed by powerful nuclease digestions that remove unprotected nucleic acids (17, 20), a strategy used to purify viruses. The level of SPHINX 1.8 DNA was still low compared with residual protected mitochondrial DNA, even with high PCR cycles (17, 20). Because we were not expecting an obvious spx1 protein signal in whole-cell homogenates, we tested whole-cell homogenates and subcellular fractions. To our surprise, the predicted spx1 band was readily detected in Western blots of GT1 cells, rodent brain, and human glioblastomas lysed in 1% Triton-PBS; to avoid off-target antibodies that are often generated by full-length proteins, we chose two peptides without any homology to mammalian sequences in the database for rabbit immunizations (*SI Materials and Methods*). Both peptides produced antibodies to the same 41-kDa band, and this band was blocked by each peptide independently confirming the identity of a correct single target. One rabbit's sera was affinity purified to label the 41-kDa band without any cross-talk. Fig. 1 shows the various whole-cell samples including control normal (NL) and GT1 cells infected with the FU-CJD agent strain isolate (lanes 1–2), NL and FU-CJD mouse brains (lanes 3–4), NL and 263K scrapie-infected hamster brains (lanes 5–6), and a frozen human glioblastoma section. Fig. 1*A* shows the many gold-stained proteins present in each lane, and Fig. 1*B* shows that the spx1 antibody highlights a major 41-kDa band in all samples. Replicate blot of samples 1–6 in Fig. 1*C* shows the spx1 blocking peptide prevented antibody binding. A second human glioblastoma (GB2) expressing the astrocyte-specific protein GFAP also showed the same 41-kDa spx1 band as shown in Fig. 1*D*. Thus, spx1 is highly conserved across mammalian species.

The spx1 band in SDS gels is ∼3.7 kDa larger than its predicted 37.3-kDa mass. It is not unusual for a protein to display a M_r on SDS-page that is different from its predicted mass, and large (10 kDa) discrepancies are often a result of glycosylation or sumoylation. Spx1 has three potential N-glycosylation sequences (N-X-S/T), but glycosidases showed it has neither N- nor O-glycosylation. In contrast, PNGase F treatment of PrP removed N-glycosylation residues but was unaffected by O-glycosidase, as predicted (Fig. 2*A* and *SI Materials and Methods*). Thus, spx1 shows no evidence of glycosylation that might account for its retarded migration. Phosphorylation typically yields multiple bands, unlike the single band detected here. There are more than 200 different posttranslational modifications that may affect gel migration, in addition to shape, other tightly bound cell components such as small peptides and lipids, and charge characteristics. Notably, spx1 has a very high percentage of strongly acidic D and E residues (20%) in its terminal 80-aa protein that could account for its gel shift (24). The presence of an iteron (replication initiation binding site) at the beginning of the 1.8 ORF might also retard its migration.

In addition to the 41-kDa band, a second minor 19-kDa band is also positive in the brain lanes loaded with more protein than the GT1 lanes. This 19-kDa band was also detected in the GT1 samples, as in the longer exposures (Fig. 3*A*, lane 1*), and the 19-kDa band was also blocked by its centrally placed peptide 1 immunogen ELDEFRKRIGVLDTEYTR (Fig. 1*C*), as well as by its more terminal C-peptide 2 RNRLSDRFKQGDESA (Fig. S1). However, whereas the 19-kDa band in mouse and hamster brains represented 4% (±0.6% SEM) of the total spx1 protein, GT1 cells consistently had a much lower percentage of this band (1%±0.4% SEM; $P < 0.005$). In sum, the spx1 antibody is highly specific for its cognate protein, and the 19-kDa band is a 41-kDa spx1 product that is significantly higher in brain than in GT1 cells.

We wanted to find out whether the spx1 protein might be differentially expressed in TSE agent-infected brains with severe neurodegeneration. To test whether spx1 was dependent on, or related to, host PrP expression and pathology, we analyzed both proteins in brains of wt mice, Tga20 mice with 8–10-fold the normal copies of PrP, and PrP null mice that are not susceptible to infection (14, 23). In addition, because limited short proteinase

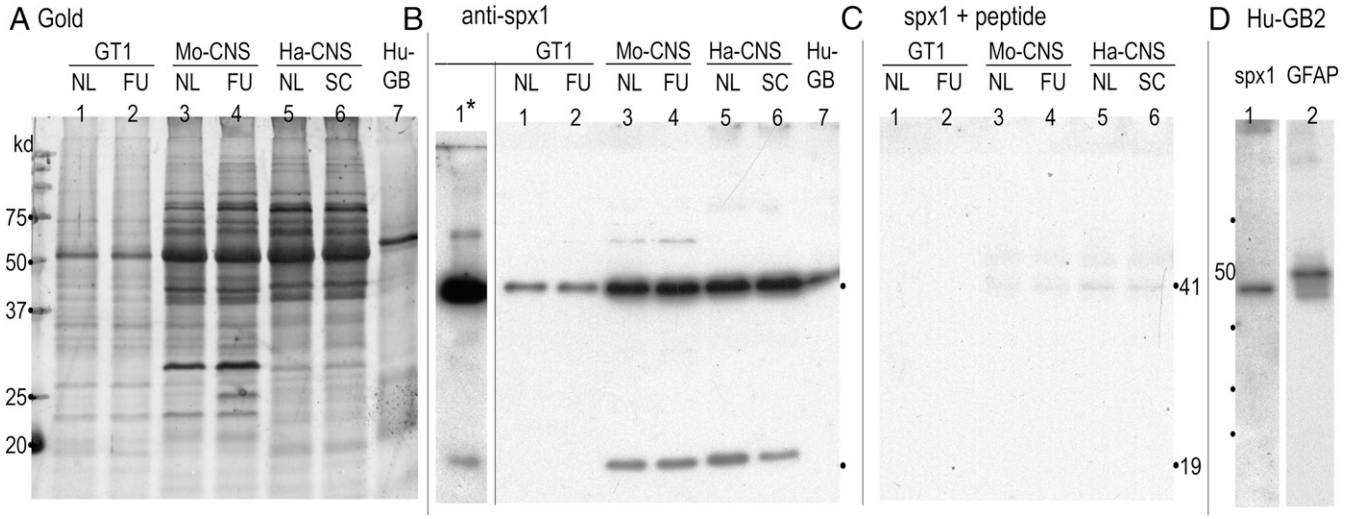

Fig. 1. Western blots of GT1 cells and brain homogenates. (*A*) Many gold-stained proteins in samples analyzed are shown. This blot was stained for gold after first detecting spx1 antibodies, as shown in (*B*), as detailed (*SI Materials and Methods*). (*B* and *C*) Replicate samples 1–6 from the same gel that was split in half for antibody (*B*) and antibody blocking (*C*) performed and detected in parallel. A major 41-kDa band is present in all control (NL) and infected GT1 cells (lanes 1 and 2), mouse brain (Mo-CNS, lanes 3 and 4), hamster brain (Ha-CNS, lanes 5 and 6) and a human glioblastoma brain sample (Hu-GB, lane 7). An additional 19-kDa spx1-positive band is seen in the central nervous system samples. The GT1 cells had much less 19-kDa band. Another gel blot of the same sample in lane 1* confirms the lower band in GT1 cells in much longer exposures. The replicate half blot of samples 1–6 (*C*) shows both bands are virtually abolished when antibody is incubated with its cognate peptide. Another glioblastoma (HuGB2; *D*) also shows the same spx1 band in addition to more abundant Glial Fibrillary Acidic protein (GFAP) in two parallel lanes separated for binding to each respective antibody. FU indicates infection with the FU-CJD agent, and SC is scrapie infection with the 263K agent strain. Marker kDa (kd) are indicated.

K (PK) digestions of whole-cell Triton lysates reveal PrP amyloid resistance (PrP-res) not seen in uninfected controls (e.g., ref. 17), it was of interest to find whether spx1 was partially resistant under the same standard digestion conditions (*SI Materials and Methods*). Parallel blots of each control and PK-treated lysates were denatured in SDS and then analyzed on blots for detection with spx1 antibody (Fig. 3*A*) and PrP antibody (Fig. 3*B*). Under these standard conditions, every NL and infected brain showed comparable amounts of PK-resistant full-length spx1, equal to 8% of undigested sample. The 19-kDa band in PK digests (PK^+ lanes in Fig. 3*A*) was significantly higher (11% ±1.2% SEM; $P < 0.0001$) than the 4% in the undigested control brains, further verifying it derives from the full-length 41-kDa band. This blot was subsequently probed with tubulin antibody as a loading control, and to confirm that unlike spx1, even at 40× loads, tubulin was completely digested (no Tu in the PK^+ lanes). Spx1 resistance was comparable in brains from the different mouse genotypes including wt (CD-1 lanes 1–4), high PrP (Tga20 lanes 5–8), and PrP null mice (lanes 9–10). In contrast, the blot in Fig. 3*B*, loaded with the same digests, shows PrP-res bands are all reduced in size and present only in infected brain. No PrP-res signal is seen in uninfected CD-1 mice (lane 2'), high PrP Tga20 mice (lane 6'), uninfected hamster (lane 12'), or PrP null mice (lanes 9'–10'). All infected brain samples (FU-CJD and scrapie-263K) showed the characteristic lower digested PrP-res band pattern. GT1 neuronal cells, as brain, consistently showed comparable resistance of the 41-kDa band (10%), but the PK digests again showed a far weaker 19-kDa signal in GT1 cells compared with brain (1% vs. 4%), as seen with its PrP counterpart in Fig. 2*B*. In sum, spx1 resistance was readily apparent and showed no relation to host PrP expression or PrP-res pathology. The reasons for spx1 resistance, and the significantly lower amounts of the 19-kDa band in GT1 cells, are not known, but one possibility is that a ligand in brain may limit digestion of some molecules.

To find out whether spx1 is compartmentalized differently in monotypic GT1 cells versus complex brain samples, we first evaluated the proportion of spx1 in crude and more purified subcellular fractions from previously characterized frozen NL and infected samples (19, 25). The only meaningful finding from these studies was that the vast majority of the spx1 protein (83%) partitioned with the 10,000 × *g* cytosol, whereas mouse and hamster brains contained 18% of the spx1 in the membrane-myelinated axon fraction that also contains many synapses and dendrites. To delineate more precisely the cellular location and

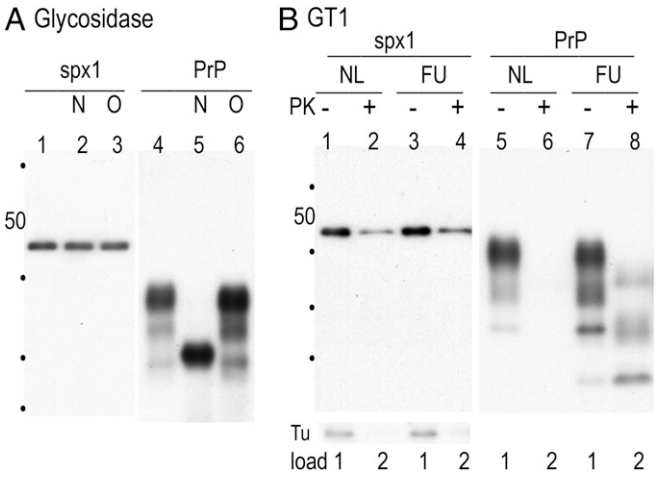

Fig. 2. Glycosylation and PK resistance of spx1. Replicate blots of mouse brain homogenates (*A*) were digested with PNGase F to remove N-linked sugars (N), or neuraminidase+O-glycosidase for O-linked sugars (O). Spx1 detection shown in lanes 1–3 and PrP in lanes 4–6. No decrease in M_r from deglycosylation is seen in spx1 digests, whereas PrP, known to have N-linked sugars, is markedly reduced in size by PNGase F (lane 5), but not O-linked digestion (lane 6), as expected. (*B*) Shows resistant spx1 in GT1 control (NL) and FU-CJD infected cells. In NL and FU-CJD samples (lanes 2 and 4, respectively), 10% of spx1 was PK resistant, whereas tubulin (Tu) showed no resistance. Parallel samples show no PrP-res in NL, whereas 25% PrP-res is seen in the FU-CJD cells (compare lanes 6 and 8).

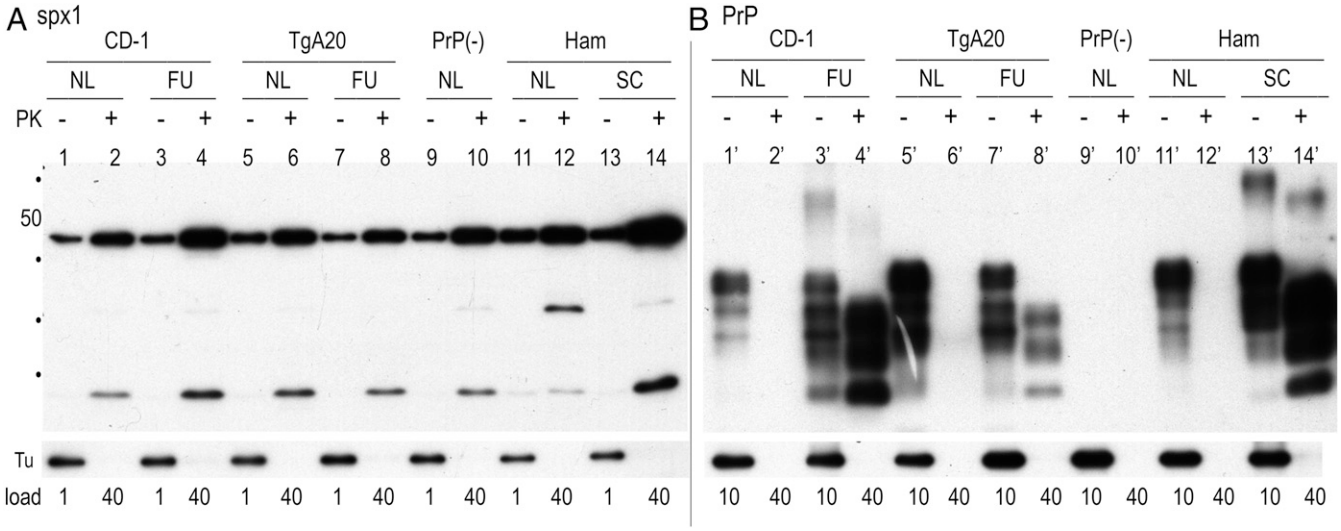

Fig. 3. Replicate blots of brain homogenates tested for PK resistance of spx1 (*A*) and PrP (*B*) on replicate blots separated for binding to antibody. Various genotypes showed ~8% resistance of full-length spx1 (PK^+ lanes) under standard digestions (*SI Materials and Methods*) in wt mice, and those with 10× PrP (Tga20), and null PrP (PrP^-). Hamster showed the same pattern, although the NL (lane 12) in this blot was a partial digest. The same samples showed PrP-res bands of reduced size only in infected brain (lanes 3, 8, and 11), and no PrP is detected in PrP null mice (lane 10). Tubulin bands in these lanes (Tu), shown at the bottom of both blots, were detected after spx1 and PrP staining and displayed no PK resistant bands. Undigested samples were loaded at 10× in the PrP blot to bring out multiple PrP bands.

potential cell type-specific expression of spx1, we pursued in situ experiments. Lightly fixed GT1 cells were permeabilized with Saponin (18; *SI Materials and Methods*). Because spx1 showed significant PK resistance, and its genomic DNA was protected, we also exposed cells to more disruptive GdnHCl treatments (*SI Materials and Methods*) that unmask hidden antigens; 2 and 3 M GdnHCl opens and inactivates many viruses, including CJD and scrapie (25). In GT1 cells, the spx1 (red signal) preferentially concentrated in the perinuclear RER-Golgi region and showed relatively low plasma membrane staining (Fig. 4). Only a faint positive signal is seen in the Saponin-only cells (Fig. 4*A*), and a stronger signal is achieved after 2 and 3 M GdnHCl unmasking (Fig. 4 *B* and *C*). Inclusion of the spx1 peptide (Fig. 4*D*) completely blocks the antibody signal, as in Western blots. No reproducible difference was seen between NL and FU-CJD-infected cells, and Fig. 4*E* at higher magnification demonstrates the intense perinuclear spx1 signal after 2 M GdnHCl unmasking.

Because rodent brains and other tissues had been fixed for several days in formalin, we used autoclaving in citrate buffer to expose buried antigens and PrP amyloid (26). This treatment also intensifies spx1 staining, consistent with a protected or masked form. Fig. 4*F* shows that spx1 is produced in a highly cell type- and tissue-specific pattern. The exocrine pancreas cells lack detectable spx1 protein, whereas the islet insulin-producing cells contain abundant spx1 protein (red). Fig. 4 *G–I* are parallel sections of representative coronal brain slices and spleen. There is negligible signal when the primary spx1 antibody is omitted (Fig. 4*G*), both brain and spleen are positive when spx1 antibody is included (Fig. 4*H*), and the spx1 signal in these tissues is completely blocked by the peptide (Fig. 4*I*). Remarkably, synaptic boutons that innervate anterior motor horn neurons are intensely stained (arrows). There is much weaker staining of RER-Golgi region of neuronal perikarya compared with cytoplasmic GT1 cell staining. The nuclei also show no spx1 signal in brain cross-sections. Note that a vessel receives no positive bouton-like structures, and that a myelinated axon is also not stained. In sum, spx1 expression is cell type- and tissue-specific, and its presence in terminal synaptic structures contrasts with its diffuse cytoplasmic pattern in the more primitive GT1 neuronal cells and specialized islet cells. These data indicate differentiation-specific processing. Additional cell and tissue-specific spx1 expression patterns in various differentiated and neoplastic cells will be reported separately, and they further support a more global role for spx1 in differentiation.

Discussion

The current experiments establish the normal mammalian expression of a 41-kDa protein that derives from a bacterial viral replication initiation homolog, rather than from any previously described mammalian nuclear, cytoplasmic, or viral sequence. SPHINX 1.8 DNA and its spx1 cognate protein do not match any known nuclear or mitochondrial sequence, nor any mammalian virus. Indeed, the possibility of new symbiotic genomes in protected cytoplasmic particles has not been widely pursued. The SPHINX 1.8 DNA showed numerous differences from representative contemporary *Acinetobacter* viruses in the database, unlike the 16-kb mitochondrial DNA extracted from particles at the same time; the latter showed 100% homology to the consensus database entry (20). Furthermore, a protein from another viral replication-initiation region of *Acinetobacter* was independently identified by deep proteomic sequencing of highly infectious CJD brain particles that lacked PrP (27). This adds to and broadens the earlier results that verify the specificity of a spx1 antibody for a replication initiation viral protein. The 41-kDa peptide migration (M_r) was close to its predicted mass, was not glycosylated, and was specifically blocked by both chosen antigenic peptides in Western blots and cytological preparations that included nontransfected neuroectodermal cells, various rodent brains, spleen and pancreatic tissues, and human glioblastoma samples. In sum, the SPHINX 1.8 DNA is clearly replicated, transcribed, and translated in selected tissues and cell types including mammalian brain, an environmentally isolated organ.

An antiserum raised elsewhere against an environmental *Acinetobacter* virus with homology to our second 2.4-kb SPHINX DNA, also isolated here from mammalian cytoplasmic particles, similarly revealed its predicted 27-kDa ORF protein in brain (17, 20). Together, these findings support the concept that other SPHINX-like circular DNAs can lurk in protected cytoplasmic particles of mammals. The finding of several different SPHINX DNAs has suggested action of more than one of these elements in concert, as well as potential helper functions in other pathologic

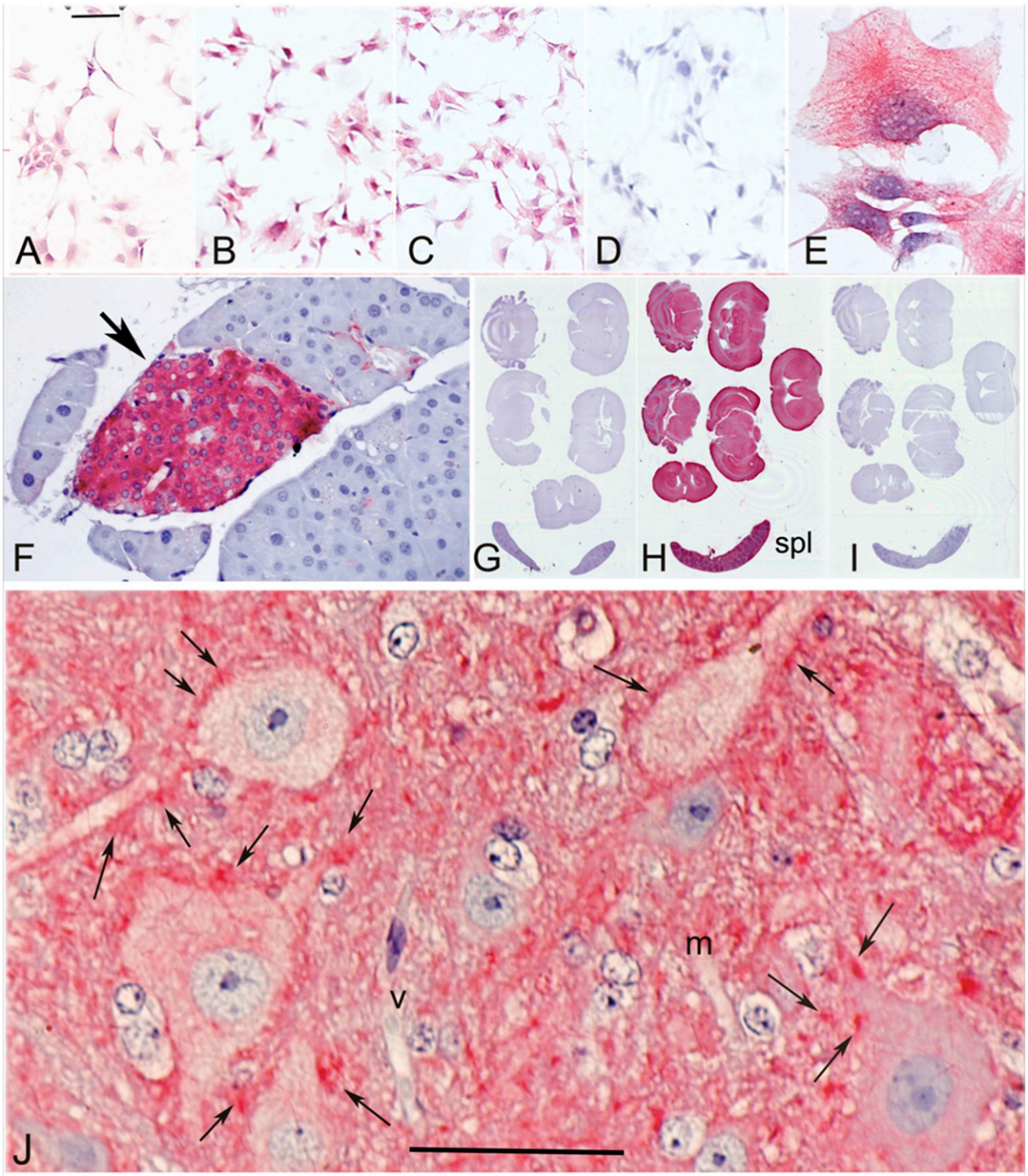

Fig. 4. Spx1 protein localization in mouse GT1 neuron derived cells (*A–E*) and spinal cord (*F*). (*A–E*) Weak but positive (red) staining in cells without GdnHCl unmasking (*A*), and more intense staining in 2 and 3 M GdnHCl-treated cells (*B* and *C*). Staining was completely blocked by the spx1 peptide (*D*), as shown in parallel stained cells first exposed to 3 M GdnHCl. (Scale bar in *A*, 100 μm, for A–D.) Higher magnification after 2 M GdnHCl treatment shows the most intense spx1 signal in perinuclear region and some fibril-like elements in the uppermost GT1 cell (*E*). Staining patterns were the same as representatively shown here in uninfected (*A–D*) and FU-CJD-infected cells (*E*). (*F*) Murine insulin-producing pancreatic islet cells (at arrow) are intensely stained, whereas exocrine pancreatic cells have no signal. (*G–I*) Slices containing five representative coronal brain sections with a spleen section at bottom (spl) treated in parallel. Omitting spx primary anitbody gave no staining in brain or spleen (*G*), showing that biotinylated secondary antibody, strepavidin alkaline phosphatase, and detector development reagents give no substantial signal. In contrast, strong positive staining is seen when the primary spx1 antibody is included (*H*). Peptide blocking again, as in GT1 cells, abolished staining of both tissue types (*I*). Mouse spinal cord (*J*) in 5-μm sections shows intense spx1 signal in synaptic boutons (arrows), many of which innervate anterior motor horn neuron dendrites and cell bodies. Nuclei lack signal (also confirmed in noncounterstained section), no labeled boutons are seen on vessels (v), and a myelinated axon (m) is also not labeled. (Scale bar, 20 μm.)

infections (20, 22). Because isolated neuronal cell lines and normal brain produce spx1, other latent circular DNA elements, including the 2.4-kb DNA, need to be further interrogated for their conservation and expression in mammalian brain and other differentiated tissues. These data also lead to the question of how this type of sequence originated, and how it is maintained.

The 1.8 (and the 2.4-kb) SPHINX DNAs both contain noncoding intervening sequences that are not in the environmental homolog, implicating an evolutionary divergence from their current environmental counterparts. The remarkable representation and concentration of spx1 in such critical structures as synapses suggests they were probably conserved on the basis of a functional advantage. Detailed tissue-specific expression and conservation of specific synaptic patterns of spx1, including ongoing studies of human brain, in addition to the current results comparing more primitive neuronal cells, brain, and pancreatic tissue, strongly indicate that spx1 is fundamentally involved in differentiation. Cellular processing of spx1 might contribute to the tissue-specific expression, and neural-derived cells showed significantly lower amounts of the 19-kDa spx1 band in GT1 cells versus brain. This was apparent in both undigested and PK^{+}-resistant preparations. A higher proportion of the cleaved 19-kDa product in brain, possibly protected by a brain-specific ligand or a conformational change, might direct spx1 to collect under terminal synaptic membranes in neurons, but not in more primitive neuronal GT1 cells. Although we have no evidence that spx1 itself is a causal factor in neurodegeneration, its location on anterior motor horn neurons that are the targets of amyotrophic lateral sclerosis encourage additional antisense strategies and clinical CSF marker studies for early diagnosis of neurodegeneration.

We propose that protected SPHINX viral elements in the environment originally invaded via wounds, or were taken up by cells in the intestinal tract after their bacterial hosts were digested by pancreatic enzymes. These viral DNAs probably persisted and spread in animals as symbiotic elements that developed into functional and essential mammalian collaborators during evolution. Because SPHINX DNAs were initially isolated from cytoplasmic particles, they probably reside and replicate in the cytoplasm, although we cannot rule out a nuclear episomal residence. Such data implicate maternal cytoplasmic inheritance, as used for the propagation of protected mitochondrial DNA.

Materials and Methods

Standard Western blots were made as previously described, and bound antibodies were developed using chemiluminescence with quantitation, as previously seen in refs. 18, 26, and 28. Archival tissues were fixed in formalin, and after unmasking, antibodies bound were developed with alkaline phosphatase detectors (23, 26, 29) (*SI Materials and Methods*). Antibodies to spx1 peptides were generated in rabbits and affinity purified by New England Peptides, as described in detail (*SI Materials and Methods*), and brain and cell fractions were made as previously (19, 25).

ACKNOWLEDGMENTS. We thank Alexander Vortmeyer for the frozen glioblastoma sections and Patrick Melich for his excellent help with the immunocytochemistry.

1. Sagan L (1967) On the origin of mitosing cells. *J Theor Biol* 14:255–274.
2. Embley TM (2006) Multiple secondary origins of the anaerobic lifestyle in eukaryotes. *Philos Trans R Soc Lond B Biol Sci* 361:1055–1067.
3. White FA, 3rd, Ishaq M, Stoner GL, Frisque RJ (1992) JC virus DNA is present in many human brain samples from patients without progressive multifocal leukoencephalopathy. *J Virol* 66:5726–5734.
4. Elsner C, Dörries K (1992) Evidence of human polyomavirus BK and JC infection in normal brain tissue. *Virology* 191:72–80.
5. Manuelidis L (1982) Nucleotide sequence definition of a major human repeated DNA, the Hind III 1.9 kb family. *Nucleic Acids Res* 10:3211–3219.
6. Manuelidis L, Biro PA (1982) Genomic representation of the Hind II 1.9 kb repeated DNA. *Nucleic Acids Res* 10:3221–3239.
7. Manuelidis L (1982) Repeated DNA sequences and nuclear structure. *Genome Evolution*, ed Flavell GDaR (Academic Press, London), Special Vol 20, pp 263–285.
8. Taruscio D, Manuelidis L (1991) Integration site preferences of endogenous retroviruses. *Chromosoma* 101:141–156.
9. Manuelidis L (1990) A view of interphase chromosomes. *Science* 250:1533–1540.
10. Chen TL, Manuelidis L (1989) SINEs and LINEs cluster in distinct DNA fragments of Giemsa band size. *Chromosoma* 98:309–316.
11. Kumar A (1998) The evolution of plant retroviruses: Moving to green pastures. *Trends Plant Sci* 3:371–374.
12. Tweedy J, et al. (2016) Complete genome sequence of germline chromosomally integrated human herpesvirus 6A and analyses integration sites define a new human endogenous virus with potential to reactivate as an emerging infection. *Viruses* 8:E19.
13. Clark DA (2016) Clinical and laboratory features of human herpesvirus 6 chromosomal integration. *Clin Microbiol Infect* 22:333–339.
14. Manuelidis L (2013) Infectious particles, stress, and induced prion amyloids: A unifying perspective. *Virulence* 4:373–383.
15. McQuaid S, Allen IV, McMahon J, Kirk J (1994) Association of measles virus with neurofibrillary tangles in subacute sclerosing panencephalitis: A combined in situ hybridization and immunocytochemical investigation. *Neuropathol Appl Neurobiol* 20:103–110.
16. Schmidt C, et al. (2015) A systematic investigation of production of synthetic prions from recombinant prion protein. *Open Biol* 5:150165.
17. Botsios S, Manuelidis L (2016) CJD and scrapie require agent-associated nucleic acids for infection. *J Cell Biochem* 117:1947–1958.
18. Manuelidis L, Yu Z-X, Barquero N, Mullins B (2007) Cells infected with scrapie and Creutzfeldt-Jakob disease agents produce intracellular 25-nm virus-like particles. *Proc Natl Acad Sci USA* 104:1965–1970.
19. Kipkorir T, Colangelo CM, Manuelidis L (2015) Proteomic analysis of host brain components that bind to infectious particles in Creutzfeldt-Jakob disease. *Proteomics* 15:2983–2998.
20. Manuelidis L (2011) Nuclease resistant circular DNAs copurify with infectivity in scrapie and CJD. *J Neurovirol* 17:131–145.
21. Whitley C, et al. (2014) Novel replication-competent circular DNA molecules from healthy cattle serum and milk and multiple sclerosis-affected human brain tissue. *Genome Announc* 2:e00849-14.
22. Zur Hausen H, Bund T, de Villiers EM (March 28, 2017) Infectious agents in bovine red meat and milk and their potential role in cancer and other chronic diseases. *Curr Top Microbiol Immunol*, 10.1007/82_2017_3.
23. Arjona A, Simarro L, Islinger F, Nishida N, Manuelidis L (2004) Two Creutzfeldt-Jakob disease agents reproduce prion protein-independent identities in cell cultures. *Proc Natl Acad Sci USA* 101:8768–8773.
24. Guan Y, et al. (2015) An equation to estimate the difference between theoretically predicted and SDS PAGE-displayed molecular weights for an acidic peptide. *Sci Rep* 5:13370.
25. Botsios S, Tittman S, Manuelidis L (2015) Rapid chemical decontamination of infectious CJD and scrapie particles parallels treatments known to disrupt microbes and biofilms. *Virulence* 6:787–801.
26. Manuelidis L, Fritch W, Xi YG (1997) Evolution of a strain of CJD that induces BSE-like plaques. *Science* 277:94–98.
27. Kipkorir T, Tittman S, Botsios S, Manuelidis L (2014) Highly infectious CJD particles lack prion protein but contain many viral-linked peptides by LC-MS/MS. *J Cell Biochem* 115:2012–2021.
28. Manuelidis L, Valley S, Manuelidis EE (1985) Specific proteins associated with Creutzfeldt-Jakob disease and scrapie share antigenic and carbohydrate determinants. *Proc Natl Acad Sci USA* 82:4263–4267.
29. Manuelidis L, Chakrabarty T, Miyazawa K, Nduom NA, Emmerling K (2009) The kuru infectious agent is a unique geographic isolate distinct from Creutzfeldt-Jakob disease and scrapie agents. *Proc Natl Acad Sci USA* 106:13529–13534.